EUKARYOTIC CELL, Sept. 2006, p. 1503–1516 Vol. 5, No. 9
1535-9778/06/$08.00+0 doi:10.1128/EC.00124-06

The Predicted G-Protein-Coupled Receptor GPR-1 Is Required for Female Sexual Development in the Multicellular Fungus *Neurospora crassa*

Svetlana Krystofova and Katherine A. Borkovich*

Department of Plant Pathology, University of California, 1415 Boyce Hall, 900 University Avenue, Riverside, California 92521

Received 28 April 2006/Accepted 30 June 2006

G-protein-coupled receptors (GPCRs) control important aspects of asexual and sexual development in eukaryotic organisms. We have identified a predicted GPCR in the filamentous fungus *Neurospora crassa* with similarity to cyclic AMP-receptor like GPCRs from *Dictyostelium discoideum* and GCR1 from *Arabidopsis thaliana*. Expression of *gpr-1* is highest in female reproductive structures, and deletion of *gpr-1* leads to defects during sexual development. Unfertilized female structures (protoperithecia) from Δ*gpr-1* strains are weakly pigmented, small, and submerged in the agar. The perithecia produced after fertilization have deformed beaks that lack ostioles, the openings through which ascospores are discharged. Localization studies using a GPR-1-green fluorescent protein fusion protein showed that GPR-1 is targeted to female reproductive structures. Genetic epistasis experiments with the three Gα genes were inconclusive due to the early block in mating exhibited by Δ*gna-1* strains. Phenotypic analysis of mutants from a high-throughput *N. crassa* knockout project allowed identification of BEK-1, a homeodomain transcription factor that is a potential target of GPR-1. The perithecial defects of Δ*bek-1* strains are similar to those of the Δ*gpr-1* strain, and epistasis analysis indicates that *bek-1* could function downstream of *gpr-1* during postfertilization events. The effect must be posttranscriptional, as *bek-1* transcript levels are not affected in Δ*gpr-1* strains. The lack of ostioles in Δ*gpr-1* and Δ*bek-1* mutants has an undesirable effect on the ability to spread progeny (ascospores) by the normal ejection mechanism and would severely compromise the fitness of these strains in nature.

In the multicellular fungus *Neurospora crassa*, sexual development is a complex process essential for survival during difficult environmental circumstances, including desiccation, heat, and nutrient deprivation. It has been shown in previous studies that formation of female reproductive structures, protoperithecia, is triggered by nitrogen starvation in *N. crassa* (reviewed in reference 62). Protoperithecia contain specialized chemotropic hyphae, termed trichogynes. Trichogynes grow toward male cells (conidia or other vegetative cells) of opposite mating type and fuse with them. The molecular mechanism of trichogyne chemotropism toward male cells is based on an interaction between pheromones secreted from male cells and cognate pheromone receptors localized in the plasma membrane of trichogynes (44, 45; H. Kim and K. Borkovich, unpublished observations). Fusion is followed by recruitment of a male nucleus to the base of the protoperithecium. The nuclei from the male and female parent recognize one another and undergo mitosis to form ascogenous hyphae. Subsequent fusion of male and female nuclei is followed by two meiotic divisions and one postmeiotic mitosis. Each resulting ascus contains eight homokaryotic, haploid ascospores. About 200 to 400 asci are encapsulated in each mature fruiting body (perithecium). Perithecia are large flask-shaped, melanized structures with a neck (beak) and ostiole (pore) at the tip through which ascospores are ejected (35). Perithecial beaks exhibit positive phototropism towards blue light (34), thus ensuring that ascospores are ejected upwards and can be spread effectively in the environment.

* Corresponding author. Mailing address: Department of Plant Pathology, University of California, 1415 Boyce Hall, 900 University Ave., Riverside, CA 92521. Phone: (951) 827-2753. Fax: (951) 827-4294. E-mail: Katherine.Borkovich@ucr.edu.

G-protein-coupled receptors (GPCRs) are seven-transmembrane helix proteins that are the sensory components of heterotrimeric G protein signaling pathways. GPCRs are crucial for the swift response to extracellular stimuli, including light, odors, hormones, neurotransmitters, and other signals (48, 53). In fungi, heterotrimeric G proteins mediate responses to environmental agents (including nutrients and pheromones) to regulate growth, colony formation, cell-cell recognition and fusion, chemotropism, mating, and cell differentiation. The early stage of mating (pheromone attraction and fusion) in *N. crassa* is regulated by pheromone receptors localized in the plasma membrane of trichogynes that sense pheromones secreted from male cells of opposite mating type (44, 45; Kim and Borkovich, unpublished). *N. crassa* has two pheromone receptors, PRE-1, expressed in *mat A* cells and PRE-2, produced by *mat a* strains (44, 45). PRE-1 and PRE-2 share homology with the *Saccharomyces cerevisiae* pheromone receptors Ste2p and Ste3p (10, 31). Pheromone receptor GPCRs are well conserved and have been reported in other fungi, including *Schizosaccharomyces pombe* (66), *Aspergillus nidulans* (65), *Ustilago maydis* (11), *Cryptococcus neoformans* (18, 21), *Schizophyllum commune* (72), and *Coprinus cinereus* (54, 56). Besides the pheromone receptors, few other groups of GPCRs have been studied in detail in fungi. Carbon source and amino acid sensing receptors have been identified and characterized in *S. cerevisiae* (75, 78, 79), *Candida albicans* (49, 50, 52), *S. pombe* (71), *C. neoformans* (74), and *N. crassa* (48a). In the homothalic fungus *A. nidulans*, a GPCR (GprD) was found to function as a negative regulator of fruiting body development (32).

Ten putative GPCRs, three G protein α subunits (GNA-1, GNA-2, and GNA-3), one Gβ subunit (GNB-1), and one Gγ subunit (GNG-1) have been identified in *N. crassa* (12, 28, 43,

TABLE 1. *N. crassa* strains used in this study

Strain	Relevant genotype	Comments[a]	Source[a]
74A-OR23-1A	Wild type, *mat A*	FGSC 987	FGSC
74a-OR8-1a	Wild type, *mat a*	FGSC 988	FGSC
*his-3*A	*his-3 mat A*	FGSC 6103	FGSC
his-3a	*his-3 mat a*		This study
3B10	Δ*gna-1*::*hph mat a*	*gna-1* homokaryon	40
A33-4	Δ*gna-2*::*pyrG*$^+$ *pyr-4 mat a*	*gna-2* homokaryon	4
31c2	Δ*gna-3*::*hph mat A*	*gna-3* homokaryon	43
20-1	Δ*gpr-1*::*bar*$^+$ *mat a*	*gpr-1* homokaryon	This study
20-2	Δ*gpr-1*::*bar*$^+$*mat A*	*gpr-1* homokaryon	This study
20-3	Δ*gpr-1*::*bar*$^+$ *mat a*	*gpr-1* homokaryon	This study
28-3	Δ*gpr-1*::*bar*$^+$ *mat a*	*gpr-1* homokaryon	This study
28-4	Δ*gpr-1*::*bar*$^+$ *mat a*	*gpr-1* homokaryon	This study
28-6	Δ*gpr-1*::*bar*$^+$ *mat A*	*gpr-1* homokaryon	This study
20-1-1	Δ*gpr-1*::*bar*$^+$ *his-3 mat A*	20-1 × *his-3 A* progeny	This study
28-6-1	Δ*gpr-1*::*bar*$^+$ *his-3 mat a*	28-6 × *his-3 a* progeny	This study
R-28-6	Δ*gpr-1*::*bar*$^+$ *gpr-1*$^+$::*his-3*$^+$ *mat A*	Complemented strain	This study
GP1GN1	Δ*gpr-1*::*bar*$^+$ Δ*gna-1*::*hph*$^+$ *mat a*	20-1 × 3B10 progeny	This study
GP1GN2	Δ*gpr-1*::*bar*$^+$ Δ*gna-2*::*pyrG*$^+$ *pyr-4 mat A*	28-6 × A33-4 progeny	This study
GP1GN3	Δ*gpr-1*::*bar*$^+$ Δ*gna-3*::*hph*$^+$ *mat a*	20-1 × 31c2 progeny	This study
G1AC1	Δ*gpr-1*::*bar*$^+$ *gna*-1(Q204L)::*his-3*$^+$ *mat A*	*gna-1*(Q204L) in Δ*gpr-1* background	This study
21-3-7	*gna-1*::*mtr*$^+$ *gna*-1(Q204L)::*his-3*$^+$ *pdx-1 mat a*	*gna-1* (Q204L) allele	76
NG22	H1-GFP::*his-3*$^+$*mat a*	H1-GFP fusion	This study
N2276	H1-GFP::*his-3*$^+$*mat A*	H1-GFP fusion	27
H1GFP	Δ*gpr-1*::*bar*$^+$ H1-GFP::*his-3*$^+$ *mat A*	H1-GFP fusion	This study
6103GFP	*gpr-1*-GFP::*his-3*$^+$ *mat A*	GPR-1-GFP fusion	This study
28-6-GFP	Δ*gpr-1*::*bar*$^+$ *gpr-1*-GFP::*his-3*$^+$ *mat A*	GPR-1-GFP fusion	This study
H4-2-2	Δ*bek-1*::*hph*$^+$ *mat A*	*bek-1* homokaryon	22
(16)A	Δ*pre-1*::*hph*$^+$ *mat A*	*pre-1* homokaryon	44
(16)a	Δ*pre-1*::*hph*$^+$ *mat a*	*pre-1* homokaryon	44
GR1PRE1A	Δ*gpr-1*::*bar*$^+$ Δ*pre-1*::*hph*$^+$ *mat A*	(16)a × 28-1 progeny	This study
GR1PRE1a	Δ*gpr-1*::*bar*$^+$ Δ*pre-1*::*hph*$^+$ *mat a*	(16)a × 28-1 progeny	This study

[a] FGSC, Fungal Genetics Stock Center, Kansas City, MO.

47, 68, 77). Loss of *gna-1* leads to trichogynes that grow randomly and are blind to males, causing female (not male) sterility in both mating types (39, 44). These observations indicate that GNA-1 is involved in the pheromone response pathway and is presumably coupled to the pheromone receptors. In contrast to Δ*pre-1* mutants which form normal protoperithecia, Δ*gna-1* strains produce fewer protoperithecia, which have abundant fringe hyphae (39). This shows that GNA-1 is also required for normal protoperithecial development. The observation that protoperithecia are normal in Δ*pre-1* mutants suggests that regulation of protoperithecial formation by GNA-1 occurs through coupling to a nonpheromone receptor GPCR. Deletion of *gna-2* or *gna-3* does not result in female sterility (4, 43, 44), and the female infertility of Δ*gnb-1* and Δ*gng-1* strains very likely results from reduced protein levels of all three Gα subunits (47, 77).

In this study, we report isolation and characterization of a putative GPCR, GPR-1, in *N. crassa*. GPR-1 is a member of a GPCR family consisting of three closely related receptors, GPR-1, GPR-2, and GPR-3 (12, 28). Deletion of *gpr-1* leads to pleiotropic phenotypic defects during sexual development. Δ*gpr-1* mutants form small, pale protoperithecia, and perithecia are frequently ruptured, lack ostioles (pores), and have defective beaks. Epistatic analysis between *gpr-1* and the three Gα genes indicates that GNA-1 may function downstream of GPR-1. Using a GPR-1-green fluorescent protein (GFP) fusion construct, we demonstrate that GPR-1 is localized in protoperithecia. In addition, we show that a homeodomain transcription factor, BEK-1, may function downstream of GPR-1 during perithecial development.

MATERIALS AND METHODS

***N. crassa* culture conditions.** *N. crassa* strains (Table 1) were maintained in Vogel's minimal (VM) medium (70). For vegetative growth, strains were cultured in either liquid VM medium with shaking (submerged cultures) or on solid VM medium, while synthetic crossing medium (SCM) (73) was used to induce formation of female reproductive structures on plates. Sorbose-containing medium (FIGS [fructose-inositol-glucose-sorbose]) was used to facilitate colony formation on plates (24). Transformants were plated using regeneration agar (17). For phosphinothricin-containing medium, the ammonium nitrate in VM or FIGS medium was replaced with potassium nitrate and 0.5% proline, and phosphinothricin was added to a final concentration of 400 μg/ml (57).

The tissue samples for RNA and protein extractions were obtained from submerged cultures, vegetative tissues grown on solid VM medium, and fertilized (perithecia) and nonfertilized (protoperithecia) female reproductive structures formed on SCM. For submerged cultures, 500 ml of liquid VM medium was inoculated with conidia from 7-day-old flask cultures at a final concentration of 1×10^6 cells/ml. Cultures were incubated in the dark at 30°C with shaking at 200 rpm for 8 or 16 h, as indicated in the figure legends. The vegetative tissues were grown in the dark at 30°C for 3 days on solid VM medium overlaid with cellophane (Bio-Rad, Hercules, CA). Protoperithecial tissues were grown on cellophane-overlaid SCM plates in constant light at 25°C for 6 days. For perithecial tissues, 6-day-old cultures grown on cellophane-overlaid SCM plates were fertilized either with the wild-type strain (heterozygous cross) or the corresponding mutant (homozygous cross) of opposite mating type and incubated for an additional 3 days under the same conditions as those used for unfertilized SCM plates.

***gpr-1* isolation and gene structure confirmation.** The *N. crassa gpr-1* gene was identified during homology searches (BLAST [1]) of the Munich Information Center for Protein Sequences (MIPS) *Neurospora* database (http://mips.gsf.de

/projects/fungi/neurospora), using the *Dictyostelium discoideum* cAR1 protein sequence, and corresponds to hypothetical gene 90c4_060. The predicted GPR-1 protein sequence is designated NCU00786.2 at the Broad Institute *Neurospora* genome database (http://www.broad.mit.edu/annotation/fungi/neurospora_crassa_7/index.html). A *gpr-1* genomic clone was isolated from the pMOcosX cosmid library (55) using PCR amplification with specific primers (GPR-1-FW and GPR-1-RV) as the screening procedure. One positive clone (G11B20) was obtained and shown to contain the *gpr-1* gene by sequence analysis (Core Sequencing Facility, Department of Microbiology and Molecular Genetics, University of Texas–Houston Medical School). Plasmids were maintained in *Escherichia coli* strain DH5α (33).

Construction of *N. crassa* strains. The *gpr-1* gene was mutated by gene replacement using the selectable marker *bar*. The *gpr-1* gene replacement vector, pSVK21, was constructed as follows. Cosmid G11B20 was digested with XbaI, and a 9-kb fragment containing the *gpr-1* open reading frame (ORF) was cloned into pBSSKII+ (Stratagene, La Jolla, CA), generating pSVK19. pSVK19 was subsequently digested with NcoI and SacI, leaving the 3-kb 3′ flank and removing the *gpr-1* ORF and 5′ region. pSVK20 contains the 1.1-kb *bar* gene (58) under the control of the *A. nidulans trpC* promoter. pSVK20 was constructed by digestion of pBARGEM-7 (58) using XbaI and SpeI to release the *bar* gene cassette. The ends of the *bar* cassette fragment were filled in using DNA polymerase I (Klenow; Promega, Madison, WI) and the blunt-end fragment was subsequently cloned into pGEM5zf digested with EcoRV to yield pSVK20. The *bar* gene cassette was excised from pSVK20 using NcoI and SacI and a 1.5-kb 5′ region of *gpr-1* from pSVK19 using SacI. The *bar* gene cassette and 1.5-kb 5′ flank of *gpr-1* were ligated into pSVK19 digested with NcoI and SacI, yielding pSVK21. The correct orientation of the *gpr-1 5′* region was verified by sequencing.

Conidia from 10-day-old cultures of *N. crassa* wild-type strain 74a (Table 1) were electroporated with 1 μg of pSVK21 linearized with EcoRI, as described previously (39, 69). Transformants were selected on FIGS medium supplemented with phosphinothricin. To identify homologous and ectopic integrations, genomic DNA was isolated from transformants, digested with KpnI, and subjected to Southern analysis (39). Genomic DNA was extracted using a Puregene kit as described by the manufacturer (Gentra Systems, Minneapolis, MN) (47). The 1.5-kb 5′ SacI-XbaI fragment from pSVK19 was labeled using the Prime-A-Gene method (Promega, Madison, WI) and used as a probe. The wild-type *gpr-1* allele produced a 6-kb hybridizing fragment during Southern analysis, while a 2.7-kb fragment was detected only in strains with homologous insertion of the bar^R cassette at the *gpr-1* locus (data not shown). Heterokaryotic strains with homologous recombination events were crossed to the wild-type strain 74A (Table 1). The progeny were selected on FIGS medium with phosphinothricin, and homokaryotic status of strains was confirmed by Southern analysis as described above.

To complement the Δ*gpr-1* mutation in *trans*, the *gpr-1* genomic clone was inserted into vector pRAUW122 and targeted to the *his-3* locus (3). The rescue plasmid pSVK22 was generated by cloning of the 9-kb XbaI fragment from pSVK19 into pRAUW122 digested with XbaI. In order to isolate a Δ*gpr-1 his-3* recipient strain, a Δ*gpr-1 mat A* strain (28-6) was crossed to a *his-3 mat a* strain (his-3a), and progeny were plated on FIGS medium supplemented with histidine and phosphinothricin. The progeny were tested for *his-3* prototrophy using VM medium without histidine. The Δ*gpr-1 his-3* strain (28-6-1) was transformed by electroporation with 1 μg of pSVK22, and transformants were plated on histidine-free FIGS medium. Genomic DNA from heterokaryons was digested with HindIII, and strains containing the wild-type *gpr-1* allele integrated at the *his-3* locus were identified by Southern analysis using the HindIII 8.8-kb *his-3* fragment excised from pRAUW122 as a probe (data not shown). Homokaryotic Δ*gpr-1*::bar^+ *gpr-1*$^+$::*his-3*$^+$ rescued strains were isolated using the microconidiation procedure (25).

Vector pMF280 contains the *N. crassa* histone H1 protein as a carboxy-terminal GFP fusion, under the control of the *ccg-1* promoter (27). Strain N2276 contains this vector targeted to the *his-3* locus in an otherwise wild-type background (27). pMF280 was also electroporated into the Δ*gpr-1 his-3* strain 28-6-1 (Table 1). Transformants were subjected to Southern analysis using the 8.8-kb HindIII fragment from pRAUW122 as a probe (see above) (data not shown), and strains with the vector integrated at the *his-3* locus were purified using the microconidiation procedure (25).

The Δ*gpr-1 his-3* strain 28-6-1 and *his-3* strains were used as recipients to produce strains expressing a GPR-1-GFP fusion protein. The pSVK52 *gpr-1*-GFP vector was constructed as follows. A 2,388-bp PCR product was amplified from pSVK19 using Turbo *Pfu* DNA polymerase (Stratagene) and Gpr1gfp-Xba-FW and Gpr1gfp-Bgl-RV oligomers designed with XbaI (5′ end) and BglII (3′ end) restriction sites. The primary blunt-end PCR product was cloned into pGEM5zf digested with EcoRV (Promega) yielding pSVK51. The 2,338-bp *gpr-1* fragment was subsequently released from pSVK51 with XbaI and BglII and cloned into *his-3* targeting vector pMF272 (27) (described above) digested with XbaI and BamHI. Ten-day-old conidia from Δ*gpr-1 his-3* strain 28-6-1 were transformed by electroporation with 1 μg of pSVK52, and transformants were plated on FIGS medium. Strains with homologous insertion of the *his-3*::*gpr-1*-GFP fragment were identified by Southern analysis of genomic DNA using the 8.8-kb HindIII fragment from pRAUW122 as a probe (data not shown). Homokaryons were purified using the microconidiation technique (25).

TABLE 2. Oligonucleotides used in this study

Name	Sequence
GPR1-INT-1-FW	5′-CGAGTTCGGACAGTACCCAACA-3′
GPR1-INT-1-RV	5′-AACCAGAGGTAGTCGCGAAAAG-3′
GPR1-INT-2-FW	5′-CTTTTCGCGACTACCTCTGGTT-3′
GPR1-INT-2-RV	5′-GCTGATGAAACACTTGATAGCC-3′
GPR1-INT-3-FW	5′-GGCTATCAAGTGTTTCATCAGC-3′
GPR1-INT-3-RV	5′-AAGAGGAAGACGAGGAGTAGTT-3′
GPR1-INT-4-FW	5′-CCAAAGATACCAGTTACCCGCT-3′
GPR1-INT-4-RV	5′-CATAACGAGCCATCCCTAATGA-3′
Gpr1gfp-Xba-FW	5′-GGTCTAGAACATFFACGACTTCATC-3′
Gpr1gfp-Bgl-RV	5′-GCAGATTAACGAGCCATCCCTACC-3′
GPR-1-FW	5′-ATCTCTCCAATCACCCAGGCTGCT-3′
GPR-1-RV	5′-TAACGAGCCATCCCTAATGACTCG-3′

Western analysis. For Western analysis, plasma membrane fractions from various tissues (see above) were isolated as described previously (68). The protein concentration was determined using the Bradford protein assay (Bio-Rad). Samples containing 25 μg of total protein were denatured and solubilized in sodium dodecyl sulfate (SDS)-polyacrylamide gel electrophoresis sample buffer (62.5 mM Tris-HCl, pH 6.8, 10% glycerol, 2% SDS, 1% β-mercaptoethanol, 0.005% bromophenol blue) by boiling for 5 min. To detect GNA-1, GNA-2, GNA-3, and GNB-1, protein samples were resolved using 10% SDS-polyacrylamide gel electrophoresis and transferred to a nitrocellulose membrane (39, 68). The primary polyclonal rabbit antibodies against GNA-1, GNA-2, GNA-3, and GNB-1 were used at dilutions of 1:1,000, 1:3,000, 1:1,000, and 1:3,000, respectively (4, 39, 43, 77). A horseradish peroxidase conjugate (Bio-Rad) was used as the secondary antibody at a dilution of 1:10,000. The blocking solution contained 5% nonfat dry milk, 25 mM Tris-Cl (pH 7.6), 140 mM NaCl, 3 mM KCl, and 0.2% Tween-20. The membranes were incubated with the primary antibody in the blocking solution for 3 h at room temperature and for 1 h with the secondary antibody. The membranes were washed four times for 5 min each time between incubations with the primary and secondary antibodies and before the application of chemiluminescence detection reagents. Detection was performed using a Biochemi system (UVP, Upland, CA) with chemiluminescence detection reagents used according to the manufacturer's protocol (Pierce, Rockford, IL).

RT-PCR analysis. In order to investigate the expression profile of *gpr-1*, total RNA was extracted from various tissues (5), and 1 μg was used in quantitative reverse transcriptase PCR (RT-PCR) (43) using the Access RT-PCR System (Promega). RT-PCR products were electrophoresed on 1.5% agarose gels, blotted onto nylon membranes, and subjected to Southern analysis as described above. The 2.4-kb *gpr-1* fragment excised from pSVK51 (XbaI-BglII) was used as the probe. The tissues used were conidia (harvested from 7-day-old flask cultures), 8- and 16-h submerged cultures, and cultures from 3-day-old VM medium plates and 6-day-old SCM plates prior to (protoperithecia) and 3 days after fertilization with opposite mating type conidia (perithecia).

Four sets of primers (Table 2) were designed to confirm the *gpr-1* gene structure predicted by the Broad Institute automated gene caller using RT-PCR (Access RT-PCR; Promega). Total RNA was extracted from 6-day-old SCM plate cultures as previously described (5), and 1 μg was used in RT-PCRs (43). Genomic intron-containing DNA controls were amplified by PCR using LA *Taq* (Takara) with cosmid G11B20 as a template. The 2.4-kb *gpr-1* fragment excised from pSVK51 (XbaI-BglII) was used as a probe.

Phenotypic analysis and microscopy. To analyze phenotypes in submerged cultures, liquid VM medium was inoculated with conidia at a final concentration of 1×10^6 cells/ml and incubated with shaking at 200 rpm for 16 h at 30°C. Apical extension rates were determined by measuring colony diameters after inoculation of 1 μl of a conidial suspension in the center of VM medium plates. The plates were incubated at 30°C in the dark, and the colony diameter was measured at 2-h intervals. Cultures were then viewed and photographed using a BX41 fluorescent microscope and C-4040 digital camera (Olympus, Lake Success, NY). Unfertilized and fertilized female reproductive tissues were cultured on SCM plates in constant light and were observed using a SZX9 stereomicroscope with

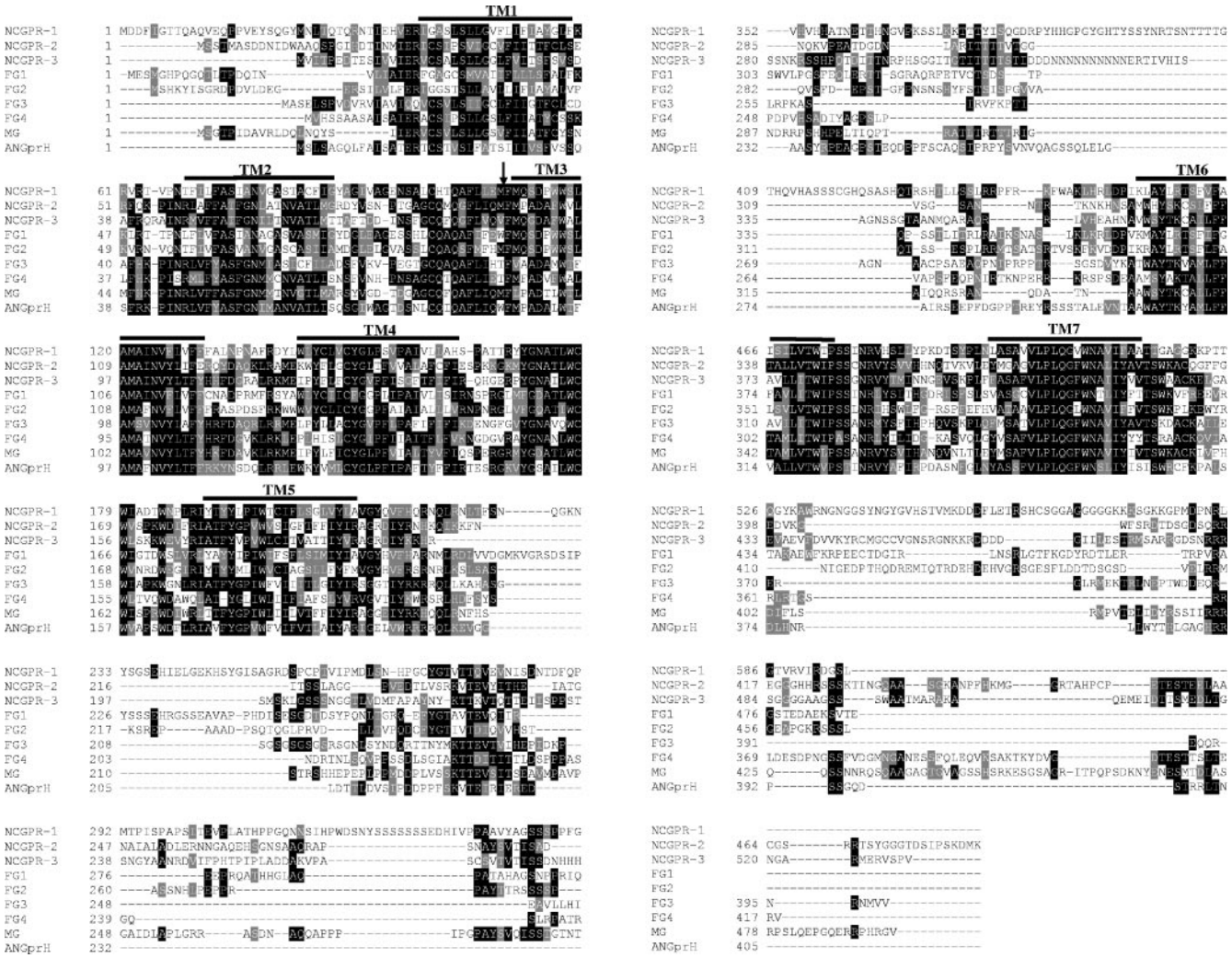

FIG. 1. Alignment of GPR-1 with other predicted fungal cAMP receptor-like GPCRs. ClustalW (http://www.ch.embnet.org/software/ClustalW.html) was used to align cAMP receptor-like GPCR protein sequences from *N. crassa* (NCGPR-1, NCU00786.2; NCGPR-2, NCU04626.2; and NCGPR-3, NCU09427.2) with predicted proteins from *M. grisea* (MG; MG06738.4), *F. graminearum* (FG1, FG09693.1; FG2, FG05239.1; FG3, FG07716.1; and FG4, FG03023.1) and *A. nidulans* (ANGprH, AN8262.2). Boxshade was subsequently used to indicate identical (black shading) and similar (gray shading) amino acid residues (http://www.ch.embnet.org/software/BOX_form.html). The bars above the sequences indicate predicted seven-helix transmembrane regions, while the arrow indicates the position of the first intron.

an ACH 1× objective lens outfitted with the C-4040 digital camera (Olympus). For microscopic observation of GFP fluorescence in strains expressing GFP fusion proteins, a BX41 fluorescent microscope with a WIB long-pass fluorescence cube (excitation 460 to 490 nm; emission 515 to 550 nm) and UM Plan Fluorite objective lenses (Olympus) was used.

For trichogyne pheromone attraction assays (7, 8, 44), cultures were grown for 6 days on 2% water agar. Chemoattraction between trichogynes and microconidia from wild-type strains was observed using a BX41 fluorescent microscope with UM Plan Fluorite objective lenses as described (44).

RESULTS

***gpr-1* identification, gene structure analysis, and expression profile.** The *gpr-1* gene was identified during BLAST (1) searches of the *N. crassa* genome at the MIPS *Neurospora* database (http://mips.gsf.de/projects/fungi/neurospora) using the cyclic AMP (cAMP) binding receptor cAR1 from *D. discoideum.* The MIPS designation is 90c4_060, while that of the Broad Institute *Neurospora* genome database (http://www.broad.mit.edu/annotation/fungi/neurospora_crassa_7/index.html) is NCU00786.2 (28). The predicted GPR-1 protein contains 596 amino acids and has a secondary structure characteristic of GPCRs, with seven transmembrane helices and a long third cytoplasmic loop and carboxy terminus (Fig. 1). GPR-1 is distantly related to the four cAMP receptors (cAR1 to cAR4) (46) and three cAMP receptor-like proteins (CrlA to CrlC) (61) from *D. discoideum*, as well as GCR1 from *Arabidopsis thaliana* (60).

Additional BLAST searches against the *N. crassa* and other fungal genomes were used to identify other ORFs with homology to GPR-1. In this way, two additional hypothetical proteins GPR-2 (NCU04626.2) and GPR-3 (NCU09427.2) were identified in *N. crassa*. The position of the second intron in GPR-2 was predicted incorrectly by the automated gene caller (data not shown). Seven amino acids (188 to 195) were removed, and the resulting protein sequence was used in the alignment. The

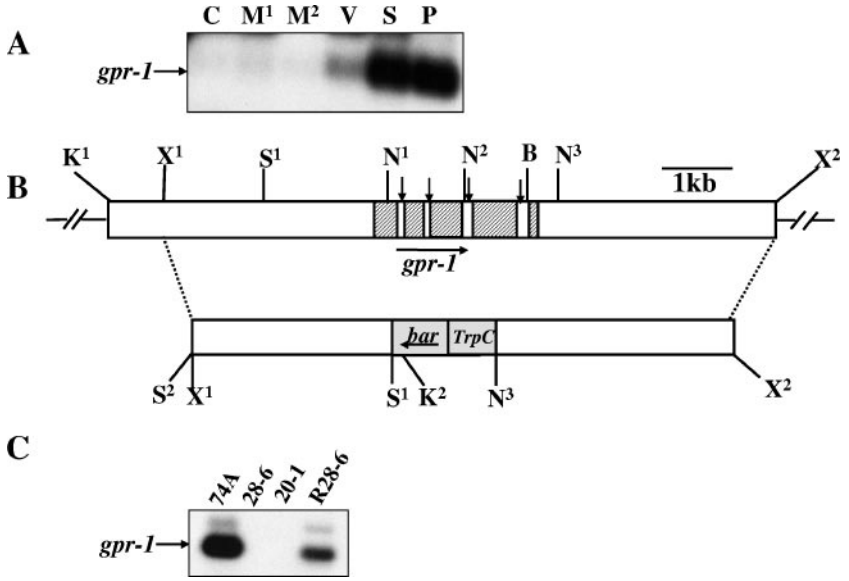

FIG. 2. Structure of the *N. crassa gpr-1* genomic region and construction of a Δ*gpr-1* strain. (A) Expression of *gpr-1* during the *N. crassa* life cycle. Total RNA was isolated from cultures of wild-type strain 74A and subjected to quantitative RT-PCR analysis as described in Materials and Methods. The tissues used were the following: C, conidia; M^1, 8-h submerged (mycelial) cultures; M^2, 16-h submerged (mycelial) cultures; V, asexual vegetative cultures grown for 3 days at 30°C in the dark on solid VM medium; S, cultures grown for 6 days on SCM plates at 25°C under light (protoperithecial cultures); and P, SCM plate cultures 3 days after fertilization with wild-type strain 74a conidia (perithecial cultures). (B) *gpr-1* genomic clone and gene replacement vector. The hatched region (top bar) indicates the *gpr-1* exons, while the vertical arrows indicate introns (white areas between exons). The gray area (bottom bar) corresponds to the phosphinothricin-resistance gene, *bar*, under control of the *A. nidulans trpC* promoter. The dashed lines illustrate the homologous recombination event leading to replacement of the *gpr-1* ORF with the *bar* cassette between the SalI (S^1) and the third NcoI sites. The horizontal arrows show the direction of transcription of *gpr-1* and *bar*. Restriction sites are as follows: N, NcoI; S, SalI; K, KpnI; B, BamHI; and X, XbaI. The second SalI site (S^2) is an artifact of cloning. (C) Verification of the *gpr-1* deletion mutant and complemented strains. Total RNA was isolated from 6-day-old protoperithecial tissues of wild type (74A), homokaryotic Δ*gpr-1* mutants (28-6 and 20-1), and a Δ*gpr-1* + *gpr-1*$^+$ complemented strain (R28-6). Levels of *gpr-1* mRNA were quantitated using RT-PCR as described in Materials and Methods. The faint, larger molecular mass species in the 74A and R28-6 samples is due to amplification of residual genomic DNA in the RNA preparations.

relatively high identity shared between GPR-1 and GPR-2 (25%) and between GPR-1 and GPR-3 (29%) indicates that these three proteins very likely form a gene family (Fig. 1).

GPCRs homologous to GPR-1 are absent from the genomes of the ascomycete yeasts *S. cerevisiae* and *S. pombe* (28). Among ascomycete filamentous fungi whose genome sequences are available, only *Fusarium graminearum* has a GPCR gene family similar to GPR-1, -2, and -3 and contains four members (24 to 36% identical to GPR-1) (Fig. 1). In contrast, *Magnaporthe grisea* and *A. nidulans* have only a single GPCR similar to GPR-1 (28% and 25% identical, respectively). The ClustalW alignment (20) (Fig. 1) shows that these proteins are similar in all seven transmembrane helices as well as in the first and second extracellular loops that are important for ligand binding. The proteins are less homologous in the third intracellular loop and the carboxy-terminal tail that are required for the physical interaction with Gα subunits. A GPCR with 27% identity to GPR-1 has been described in the basidiomycete yeast *C. neoformans* (Gpr4) (74) and is implicated in sensing the amino acids proline and methionine.

The predicted gene structure of *gpr-1* contains five exons and four introns (Fig. 2B). The presence of the introns was confirmed by RT-PCRs using four sets of oligonucleotides (Table 2) designed within the exons that flank each intron. Total RNA was used as the template in RT-PCR, whereas the genomic cosmid clone G11B20 was used for amplification of genomic fragment controls using the same sets of primers. The RT-PCR and genomic DNA PCR products were subjected to Southern analysis. The analysis confirmed the presence and sizes of the four introns as predicted by the automated gene caller (Fig. 2B) (data not shown). The *A. nidulans gprH* gene (Fig. 1) also contains four predicted introns (http://www.broad.mit.edu/annotation/fungi/aspergillus). In contrast, other GPR-1-related GPCRs have two predicted introns in their ORFs at very similar or identical positions as GPR-1. In particular, the position of the first intron is highly conserved in all GPR-1-related GPCRs and is located at the junction of the first extracellular loop and the third transmembrane helix (Fig. 1).

gpr-1 mRNA levels are too low to detect by Northern analysis (data not shown). Therefore, quantitative RT-PCR was performed to determine the expression of *gpr-1* during various developmental stages. Detectable levels of *gpr-1* mRNA were present in three tissues: vegetative plates and protoperithecial and perithecial tissues (Fig. 2A). Highest expression was observed in the two sexually differentiated tissues. The relative amounts of *gpr-1* in protoperithecial and perithecial cultures were comparable, suggesting that *gpr-1* may function during pre- and postfertilization events in *N. crassa*.

Δ*gpr-1* strains exhibit phenotypic defects during sexual development. A Δ*gpr-1* mutant was isolated after electroporation of a wild-type strain with a construct in which the *gpr-1* coding region was replaced with a phosphinothricin resistance gene

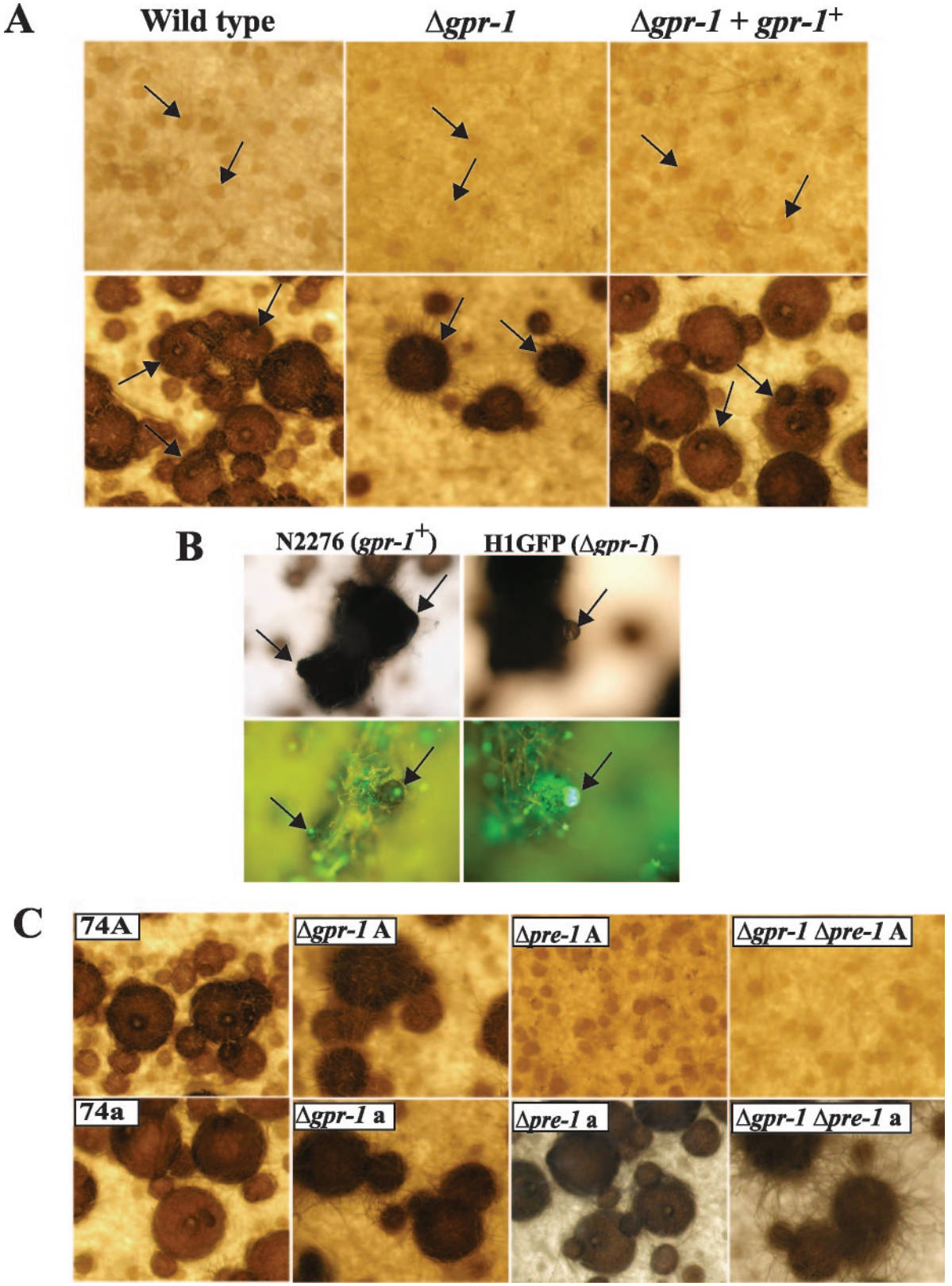

FIG. 3. Phenotypic characterization during the sexual cycle. (A) Unfertilized (protoperithecia) and fertilized (perithecia) structures. Strains were cultured on solid SCM at 25°C for 6 days in light (top panels; protoperithecia). At this time, half of the plate was fertilized with wild-type conidia of opposite mating type (74a or 74A) and photographed 3 days after fertilization (bottom panels; perithecia). For the analysis, wild-type (74A), Δ*gpr-1* (28-6 and 20-1), and Δ*gpr-1* + *gpr-1*$^{+}$ (R28-6) strains were used. Arrows indicate protoperithecia (top panels) or perithecia (bottom panels; enlarged dark bodies). Photographs were taken at ×25 magnification. (B) Microscopic images of perithecial beaks. Strains expressing

cassette (Fig. 2B) (58). Heterokaryotic primary transformants were obtained by selection on medium containing phosphinothricin (see Materials and Methods for details). Strains with the proper homologous recombination event were crossed to a wild-type strain of opposite mating type in order to produce homokaryotic Δ*gpr-1* mutant ascospore progeny (data not shown). The purity of homokaryons was verified by Southern analysis (data not shown), and RT-PCR analysis confirmed that homokaryotic Δ*gpr-1* strains lack *gpr-1* mRNA (Fig. 2C). The Δ*gpr-1* mutation was complemented in *trans* with the original 9-kb *gpr-1* genomic fragment targeted to the *his-3* locus (see Materials and Methods). The restoration of *gpr-1* mRNA expression in Δ*gpr-1* + *gpr-1*$^+$ complemented strains was confirmed by RT-PCR (Fig. 2C).

Δ*gpr-1* strains were analyzed for phenotypes during the life cycle. Δ*gpr-1* mutants do not possess any obvious defects during asexual growth or development (data not shown). Traits tested included hyphal extension rate under normal and hyperosmotic conditions and various aspects of macroconidiation. Consistent with the results from expression profile analysis showing that *gpr-1* mRNA levels are highest in unfertilized and fertilized female tissues, deletion of *gpr-1* leads to several defects during sexual development. Protoperithecia are weakly pigmented, and a significant number are small and submerged in the agar during growth on solid medium (Fig. 3A). Perithecia from Δ*gpr-1* mutants possess a significantly greater number of fringe hyphae on the surface in comparison to the wild-type strain, giving them a "hairy" appearance. The abundant formation of fringe hyphae has been reported previously in Δ*gna-1* strains (39) (see below). The underlying cause of this phenomenon, which has been observed in other mutants with defects in sexual reproduction, is not known. The Δ*gpr-1* perithecia have deformed beaks and lack ostioles (pores) at the tips that are essential for appropriate ejection of ascospores. Moreover, they are frequently ruptured, leading to the release of the perithecial contents (Fig. 3A and B; see also Fig. 6B). In contrast to wild type, significantly fewer perithecia reach maturity in Δ*gpr-1* mutants (Fig. 3A). Those Δ*gpr-1* perithecia that are fully developed produce a similar number of ascospores as wild-type strains. The viability of ascospores was identical to that of wild type during both homozygous and heterozygous crosses (data not shown). Δ*gpr-1* + *gpr-1*$^+$ rescued strains are phenotypically identical to wild type (Fig. 3A and B), confirming that the defects of Δ*gpr-1* mutants result from loss of the *gpr-1* gene product.

In order to better observe ascospore emergence from perithecia, we analyzed strains containing a histone H1-GFP fusion protein under the control of *ccg-1* promoter (see Materials and Methods). Previous studies have shown that this GFP fusion allows clear visualization of ascospores, due to the strong fluorescence of the H1-GFP protein in their nuclei (27). Microscopic analysis of strains expressing the H1-GFP fusion protein confirmed the morphological differences observed in wild-type *gpr-1*$^+$ (N2276) and Δ*gpr-1* mutant (H1GFP) strains with regard to missing ostioles and ruptures in the perithecial wall (Fig. 3B). Fluorescence from ascospores within intact perithecia was observed through the ostiole in wild type (Fig. 3B). In contrast, perithecia from Δ*gpr-1* mutants are ruptured, with ascospores oozing from the fissures in the structure (Fig. 3B).

GPR-1 is not the only GPCR that is highly expressed during sexual development in *N. crassa*. A previous study has shown that the pheromone receptor gene *pre-1* is present at high levels in both protoperithecial and perithecial tissues (44). Deletion of *pre-1* in a *mat A* background leads to defective chemoattraction towards *mat a* males, subsequently resulting in a complete block in cell fusion and perithecial development (44). The trichogyne attraction assay was used to investigate the possibility that Δ*gpr-1* strains might also be affected during early stages of mating. Chemotropism of trichogynes toward male cells of opposite mating type, as well as the ability of male cells (conidia) to attract trichogynes of opposite mating type, were not disrupted in Δ*gpr-1* strains (data not shown). This result indicates that although PRE-1 and GPR-1 are highly expressed during sexual development, they very likely regulate different events. Furthermore, contrary to *pre-1*, *gpr-1* expression is not mating-type specific (data not shown). We further probed the relationship between *pre-1* and *gpr-1* through analysis of Δ*gpr-1* Δ*pre-1* double mutants (Fig. 3C). Δ*gpr-1* Δ*pre-1* strains possessed the defects of both single mutants, confirming independent roles for these receptors during sexual development (Fig. 3C). The Δ*gpr-1* Δ*pre-1* double mutants formed fewer protoperithecia than wild-type or Δ*gpr-1* strains, and protoperithecia from the double mutants were "hairy." The *mat A* Δ*gpr-1* Δ*pre-1* mutants did not form perithecia after fertilization with *mat a* males, reflecting the absence of PRE-1. Conversely, the *mat a* Δ*gpr-1* Δ*pre-1* strains formed perithecia without ostioles after fertilization with *mat A* males, indicating the loss of GPR-1. Thus, PRE-1 is essential for cell-cell recognition and fusion, while GPR-1 is required for normal development of unfertilized (protoperithecial) and fertilized (perithecial) female structures.

Epistasis analysis between *gpr-1* and the three *N. crassa* Gα subunits. Previous work has demonstrated that the Gα subunit GNA-1 (39, 44) and Gβγ dimer GNB-1/GNG-1 (44, 47, 77) are essential for female (but not male) fertility in *N. crassa.* The functions of these proteins are mating type independent, since they are required downstream of both pheromone receptors (PRE-1 and PRE-2) in *mat A* and *mat a* strains, respectively (44; Kim and Borkovich, unpublished observations). Trichogynes of Δ*gna-1*, Δ*gnb-1*, and Δ*gng-1* mutants exhibit

a histone H1-GFP fusion protein, N2276 (*gpr-1*$^+$ strain) and H1GFP (Δ*gpr-1* strain), were cultured on SCM plates for 6 days and then fertilized with opposite mating type conidia. Seven days later, perithecia were subjected to phase-contrast microscopy (upper panels) and detection of GFP fluorescence (bottom panels) (see Materials and Methods). Images are shown at ×200 magnification. The arrows indicate perithecial beaks (left panels) or ruptured perithecia (right panels). (C) Epistasis analysis between *gpr-1* and *pre-1*. Strains were cultured to produce perithecia as indicated in panel A. Wild-type *mat A* (74A) and *mat a* (74a), Δ*gpr-1 mat A* (28-6; Δ*gpr-1*A), Δ*gpr-1 mat a* (20-1; Δ*gpr-1* a), Δ*pre-1 mat A* [(16)A; Δ*pre-1* A], Δ*pre-1 mat a* [(16)a; Δ*pre-1* a], Δ*gpr-1* Δ*pre-1 mat A* (GR1PRE1A; Δ*gpr-1* Δ*pre-1* A), and Δ*gpr-1* Δ*pre-1 mat a* (GR1PRE1a; Δ*gpr-1* Δ*pre-1* a) strains were used for analysis. Photographs were taken at ×25 magnification.

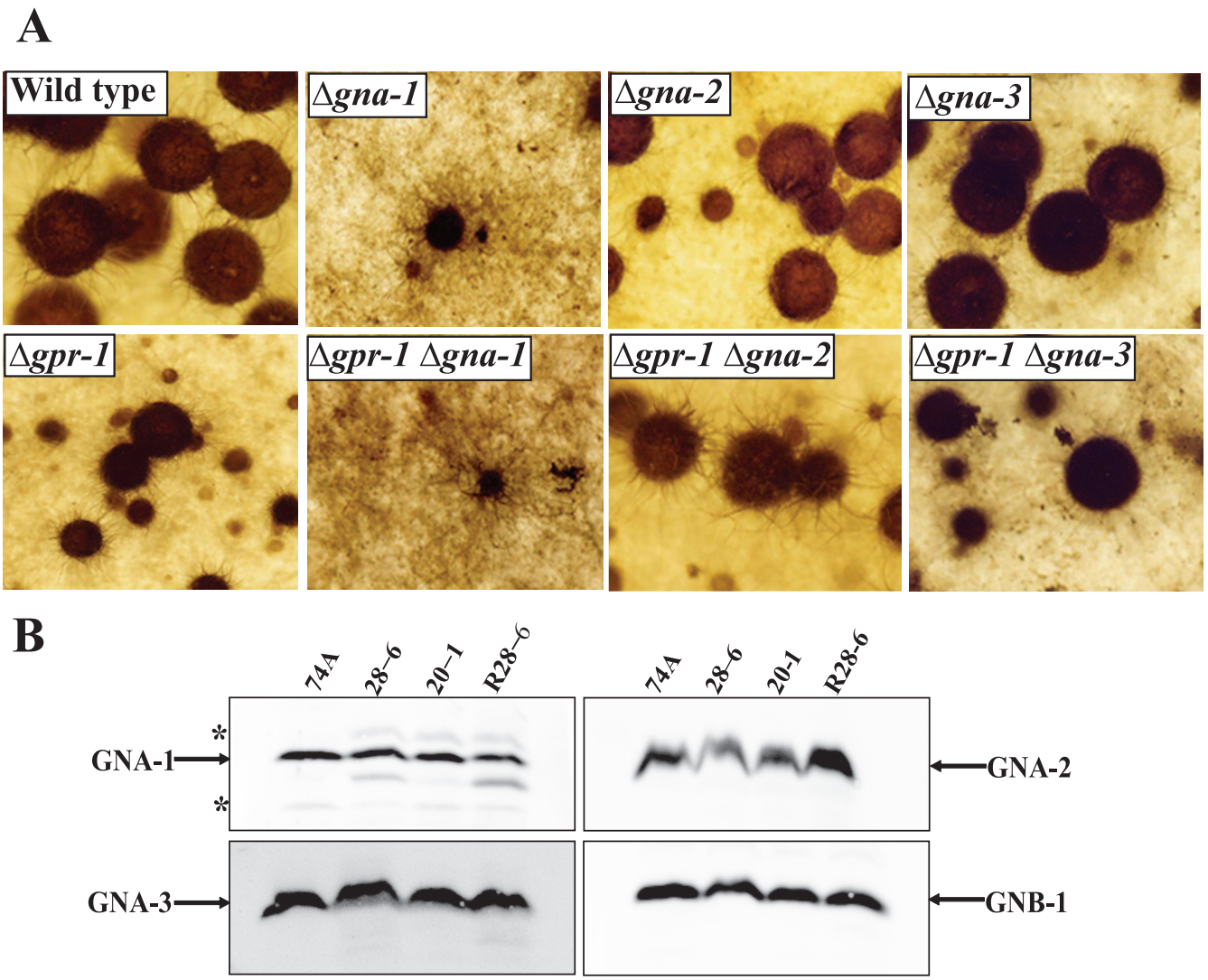

FIG. 4. Relationship between GPR-1 and G protein subunits. (A) Epistasis analysis between *gpr-1* and the three Gα genes. Strains were cultured to produce perithecia as indicated in the legend of Fig. 3A. Wild-type (74A), Δ*gpr-1* (28-6), Δ*gna-1* (3B10), Δ*gna-2* (A33-4), Δ*gna-3* (31c2), Δ*gpr-1* Δ*gna-1* (GP1GN1), Δ*gpr-1* Δ*gna*-2 (GP1GN2), and Δ*gpr-1* Δ*gna-3* (GP1GN3) strains were used for analysis. Photographs were taken at ×25 magnification. (B) Analysis of Gα and Gβ protein levels. The plasma membrane fraction was isolated from SCM plate cultures, and samples containing 25 μg of protein were subjected to Western analysis using specific antisera (see Materials and Methods). Wild-type (74A), Δ*gpr-1* (28-6 and 20-1), and Δ*gpr-1* + *gpr-1*$^{+}$ (R28-6) strains were used for analysis. The asterisks indicate nonspecific bands.

severe defects in chemoattraction and fusion with male cells, similar to those of Δ*pre-1 mat A* strains (44, 47). It has been hypothesized that GNA-1 is the Gα subunit that communicates the pheromone signal from PRE-1 to downstream effectors (44). During homozygous crosses, Δ*gna-3* strains form a large number of perithecia with short beaks that are embedded in the agar medium (43; data not shown). Such crosses also produce a large proportion of nonviable ascospores. The Δ*gna-2* mutant has no obvious defects during either asexual or sexual development, but Δ*gna-1* Δ*gna-2* and Δ*gna-2* Δ*gna-3* double mutants have more severe defects than strains lacking only *gna-1* or *gna-3* (4, 42).

The results demonstrate that *gpr-1* is required for normal perithecial development, but the phenotype of Δ*gpr-1* strains differs from that observed in the single Gα mutants. Therefore, we explored functional relationships between GPR-1 and the three Gα proteins through examination of protoperithecial and perithecial development in Δ*gpr-1* Gα single and double mutants. Δ*gna-1* strains form "hairy" protoperithecia that enlarge slightly after fertilization but fail to develop mature perithecia. This phenotype is similar to that observed for fringe hyphae production in perithecia of Δ*gpr-1* mutants (Fig. 4A). The Δ*gpr-1* Δ*gna-1* double mutant exhibits phenotypic defects identical to those of the Δ*gna-1* mutant during protoperithecial and perithecial development, leaving open the possibility that GNA-1 is coupled to GPR-1 (Fig. 4A). However, since the other two Gα subunits are also implicated in sexual development, we could not exclude the possibility that either GNA-2 or GNA-3 might be coupled to GPR-1 at a certain time during sexual development. The Δ*gpr-1* Δ*gna-2* strain has defects identical to those observed in Δ*gpr-1* single mutants (Fig. 4A), but the epistatic relationship is unclear due to the absence of

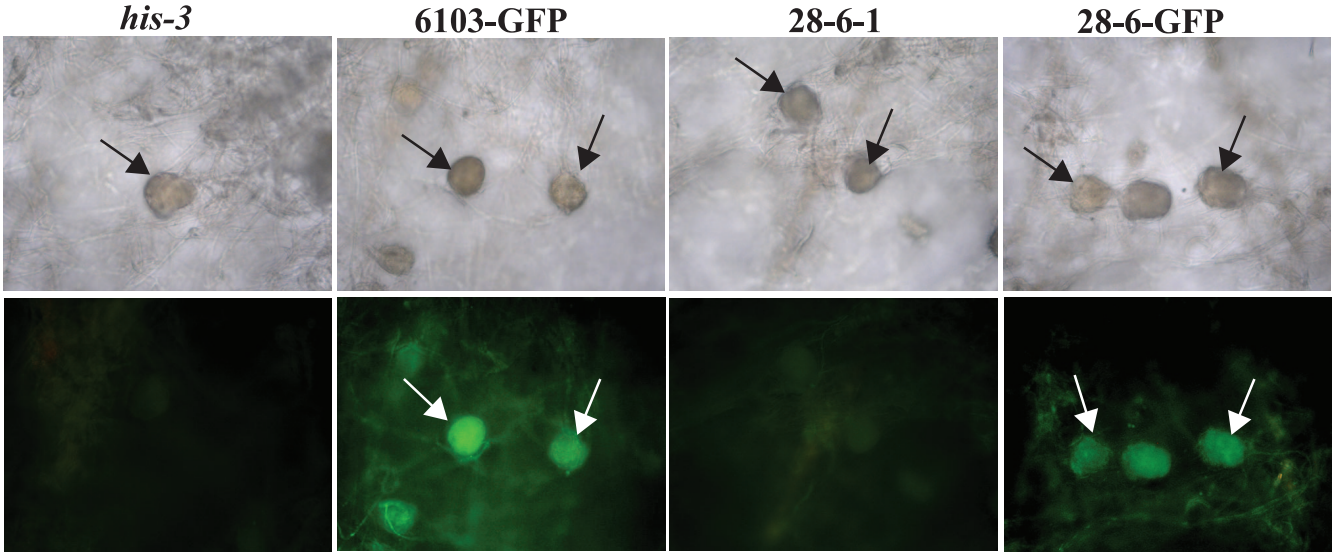

FIG. 5. Localization of a GPR-1-GFP fusion protein. Phase-contrast (upper panels) and GPR-1-GFP localization (bottom panels) images from 6-day-old unfertilized SCM tissues were obtained as described in the legend of Fig. 3B. Strains carrying *gpr-1*$^+$ (*his-3*) and Δ*gpr-1* (28-6-1) untransformed controls or those expressing a GPR-1-GFP fusion protein in the *gpr-1*$^+$ (6103-GFP) or Δ*gpr-1* (28-6-GFP) strain background were used for analysis. Images are shown at ×200 magnification. Arrows indicate protoperithecia.

phenotypes in Δ*gna-2* single mutants. Similar to Δ*gpr-1* strains, Δ*gpr-1* Δ*gna-3* mutants form small perithecia with no ostioles. However, perithecia from Δ*gpr-1* Δ*gna-3* mutants also have short beaks, like Δ*gna-3* strains (Fig. 4A). The phenotype of Δ*gpr-1* Δ*gna-3* mutants is a combination of both gene mutations, and therefore the epistatic analysis does not support coupling between GNA-3 and GPR-1 during perithecial development.

Since the epistasis analysis between *gpr-1* and the Gα genes ruled out GNA-2 and GNA-3 as downstream effectors of GPR-1 but left open the possibility that GNA-1 is coupled to GPR-1, we examined whether constitutive activation of *gna-1* could bypass the defects of the Δ*gpr-1* mutation. The predicted GTPase-deficient, dominant-activated *gna-1*(Q204L) allele construct (76) was targeted to the *his-3* locus of a Δ*gpr-1 his-3* strain, and transformants were selected and purified as described in Materials and Methods. Δ*gpr-1* strains expressing the dominant-activated *gna-1* allele showed an even greater reduction in perithecial formation than observed in Δ*gpr-1* strains, but ostiole production was not recovered (data not shown). This outcome indicates that activation of GNA-1 alone cannot rescue the perithecial defects of strains lacking GPR-1.

To elucidate whether deletion of *gpr-1* affects G protein levels, we performed Western analysis using specific antibodies raised against individual G protein subunits (4, 39, 43, 77). The results show that the three Gα proteins, GNA-1, GNA-2, and GNA-3, and the Gβ protein, GNB-1, are present at the same level in Δ*gpr-1* and wild-type strains (Fig. 4B). Thus, the presence of *gpr-1* has no effect on the concentration of G protein subunits associated with the plasma membrane, supporting the proposal that the aberrations observed during sexual development in Δ*gpr-1* mutants result from loss of GPR-1.

GPR-1 is localized in female reproductive structures. The phenotypic defects identified during sexual development in Δ*gpr-1* strains are consistent with the high expression of *gpr-1* in female reproductive structures. To determine whether GPR-1 localization correlates with the presence of *gpr-1* mRNA, we constructed strains that express a carboxy-terminal fusion of GFP to GPR-1. The fusion vector was transformed into *his-3* and Δ*gpr-1 his-3* strains, and transformants with homologous recombination events at the *his-3* locus were isolated (see Materials and Methods). The GPR-1-GFP fusion protein did not have any obvious effect on sexual development in the wild-type background and was able to partially complement the defects of the Δ*gpr-1* mutant (data not shown). Since perithecia are heavily melanized, we focused on microscopic observation of unfertilized female reproductive tissues. Fluorescence was observed in protoperithecia of strains containing the GPR-1-GFP fusion, consistent with localization of GPR-1 in this structure (Fig. 5).

BEK-1 is a homeodomain transcription factor that functions downstream of GPR-1. BEK-1 is a homeodomain transcription factor protein (NCU00097.2) previously annotated in the *N. crassa* genome sequence (12). Typically, homeobox proteins contain a ~60-amino-acid long homeodomain sequence (30). BEK-1 is similar to members of the TALE (three-amino-acid loop extension) superfamily of atypical homeodomain transcription factors characterized by an extension of three amino acids between two α helices within the homeodomain (16). This extension almost always consists of proline-tyrosine-proline (PYP) and is followed by a serine or threonine and several acidic residues (16). These amino acids are crucial for the interaction with other homeobox proteins, such as PBX and HOX (29). Members of the TALE family include MEIS (myeloid ecotropic viral insertion sites), TGIF, PBX, and IRO (Iroquois) in animals, KNOX and BEL in plants, and M-ATYP and CUP in fungi (16). Alignment analysis of the homeodomain regions of BEK-1 with members of the TALE family revealed that BEK-1 shares high identity (53 to 77%) with the homeodomains of these proteins and confirmed that

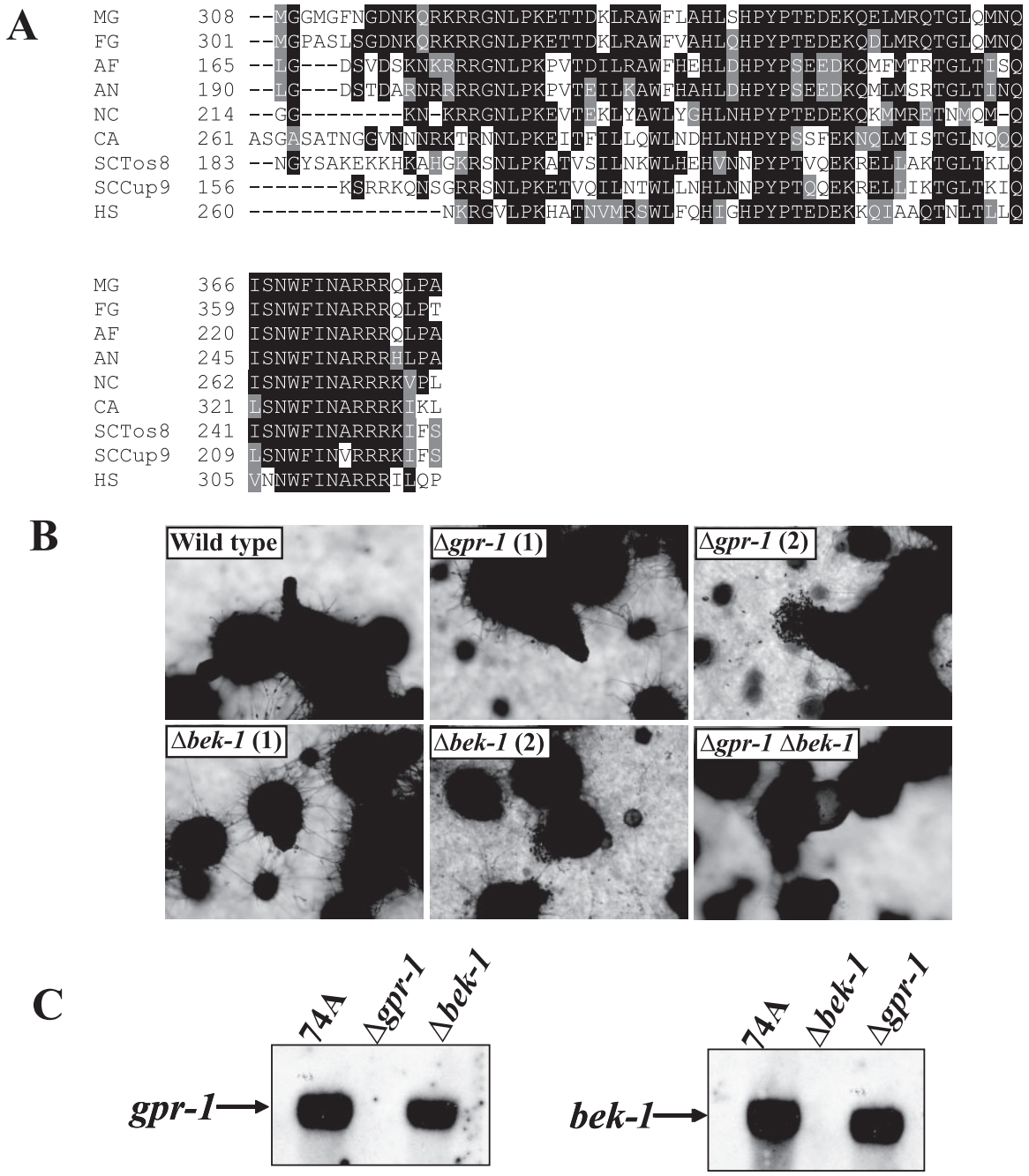

FIG. 6. Epistasis analysis between *gpr-1* and *bek-1*. (A) Alignment of BEK-1 with related homeodomain transcription factors. ClustalW (http://www.ch.embnet.org/software/ClustalW.html) was used to align *N. crassa* BEK-1 (NC; NCU00097.2) with putative homeodomain transcription factors from the fungi *F. graminearum* (FG; FG05475.1), *A. fumigatus* (AF; Afu4g10110), *A. nidulans* (AN; AN2020.2), and *C. albicans* (CA; CaJ7.0235) and previously characterized homeodomain proteins identified as *M. grisea* Pth12p (MG; DQ060925.1), *S. cerevisiae* Tos8p (SCTos8; YGL096W) and Cup9p (SCCup9; YPL177C), and human PKNOX1 (HS; accession number AAC51243). Boxshade was used to indicate identical (black shading) and similar (gray shading) amino acid residues (http://www.ch.embnet.org/software/BOX_form.html). (B) Perithecial development. Perithecia from wild-type (74A), Δ*gpr-1* (28-6), Δ*bek-1* (BK1), and Δ*gpr-1* Δ*bek-1* (GP1BK1) strains were analyzed microscopically 6 days after fertilization. Images were captured at ×52 magnification. Two images were taken for Δ*gpr-1* and Δ*bek-1* strains, showing perithecial defects (1) and ruptured perithecia (2). (C) Expression of *gpr-1* and *bek-1*. Total RNA was isolated from perithecial tissues of wild-type (74A), Δ*gpr-1* (28-6), and Δ*bek-1* (BK1) strains 3 days after fertilization and subjected to quantitative RT-PCR as described in Materials and Methods.

BEK-1 contains the PYP motif in the same position as other proteins in the TALE superfamily (Fig. 6A).

A Δ*bek-1 N. crassa* mutant was created during a high-throughput reverse genetics project (22). In contrast to results with Δ*gpr-1* mutants, there were no visible protoperithecial defects in Δ*bek-1* strains. However, the Δ*bek-1* mutant shares several defects in common with Δ*gpr-1* strains during perithecial development. The *bek-1* mutant forms small, "hairy" peri-

thecia that are frequently ruptured, and these perithecia also lack ostioles (Fig. 6B). However loss of *bek-1* results in more severe deformation of perithecial beaks than observed in Δ*gpr-1* strains. Perithecia from Δ*bek-1* strains have very short beaks (Fig. 6B), while those from Δ*gpr-1* mutants form volcano-shaped beaks during later stages of perithecial development. The more severe defects observed in the Δ*bek-1* mutant could result from a convergence of multiple signal transduction pathways, including GPR-1, that regulate BEK-1 function. To corroborate a possible functional relationship between GPR-1 and BEK-1, Δ*gpr-1* Δ*bek-1* double mutants were isolated. Δ*gpr-1* Δ*bek-1* strains exhibit defects very similar to those observed in the Δ*bek-1* mutant, consistent with BEK-1 functioning downstream of GPR-1 during perithecial development. The mechanism by which GPR-1 regulates BEK-1 is not currently known. However, deletion of *gpr-1* does not greatly affect expression of *bek-1*, and loss of *bek-1* does not lead to a significant reduction in *gpr-1* mRNA levels, indicating that any regulation of BEK-1 function by GPR-1 is posttranscriptional (Fig. 6C).

DISCUSSION

N. crassa GPR-1 is the first cAMP receptor-like (CRL) GPCR characterized in ascomycete fungi. GPR-1 is differentially expressed, and the highest expression was detected during development of female reproductive structures, before and after fertilization. Deletion of *gpr-1* leads to several phenotypic defects during sexual development. Although Δ*gpr-1* strains are not female sterile, their ability to disperse progeny is severely compromised. This is caused by the absence of ostioles at the tip of the perithecium through which mature ascospores are discharged.

Fungal GPCRs have been divided into four major groups: (i) the pheromone-sensing receptors Ste2 and Ste3 of *S. cerevisiae*, (ii) the glucose sensing Gpr1 receptor of *S. cerevisiae*, (iii) the putative nutrient sensing receptor Stm1 of *S. pombe*, and (iv) proteins related to the CRL receptors of *D. discoideum* (12, 28, 32). A fifth group of seven-helix proteins, the microbial opsins, have not been implicated in G protein signaling in fungi (6; data not shown). The CRL receptors constitute a functionally divergent group of GPCRs that are similar to cAMP receptor GPCRs from *D. discoideum*. In *N. crassa*, this receptor group consists of three proteins (GPR-1, GPR-2, and GPR-3). *A. nidulans* and *M. grisea* have only one CRL-related protein, while *F. graminearum* contains four CRL receptors (Fig. 1). The related protein from *A. nidulans*, GprH, has been described previously, but no function has yet been assigned (32).

CRL GPCRs have been characterized phenotypically in slime mold *D. discoideum* (61) and the model plant *A. thaliana* (19, 23, 41, 60). Although CRL GPCRs are absent from both budding and fission yeasts, proteins with weak similarity to this group of receptors have been identified in the basidiomycete *C. neoformans* (74). Despite their sequence homology, CRL receptors appear to have very diverse functions in different species. For example, although *N. crassa* GPR-1, GPR-2, and GPR-3 possess significant amino acid identity, our analysis indicates that GPR-1 does not share any obvious functions with GPR-2 or GPR-3 (S. Krystofova and K. A. Borkovich, unpublished observations). In *D. discoideum*, the CrlA receptor functions as a negative regulator of cell growth and appears to be required for prestalk cell differentiation (61). GCR1 is the only characterized GPCR from *A. thaliana* and physically interacts with the lone *A. thaliana* Gα protein, GPA1 (59). Previous studies investigating loss-of-function or overexpression *gcr1 A. thaliana* lines, as well as in vitro experiments with BY2 tobacco cell cultures, showed that GCR1 is required for seed germination and that GCR1 regulates DNA synthesis through activation of phosphatidylinositol-specific phospholipase C (2, 19, 23). Deletion of the CRL-related gene *gpr4* in *C. neoformans* leads to modest defects in cell fusion during mating and reduced capsule formation (74).

The shared sequence homology of CRL proteins in ascomycete fungi is distributed in both extracellular and transmembrane regions, suggesting that these GPCRs share structural or functional similarity, e.g., by responding to similar stimuli (ligands) or coupling to comparable downstream components. In addition, we examined the correlation between intron positions and secondary protein structure in this group of GPCRs. In our previous studies, we reported that the position of introns in heterotrimeric G protein genes (Gα and Gγ subunits) was highly conserved in mammals and *N. crassa* (47, 68). Since mammalian GPCRs are for the most part intronless (14) and do not contain receptors related to GPR-1, we compared gene structure only within the cAMP receptor-like family present in ascomycete fungi (Fig. 1). These receptors share a very similar gene structure in which introns are found only in nontransmembrane regions. It is worthwhile to point out that the position of the first intron in all genes presented in our study is highly conserved and located at the junction of the first extracellular loop and the third transmembrane region (Fig. 1). The evolutionary significance of the presence of an intron in a highly conserved region of these proteins has not yet been established. The large number of GPCRs identified in *N. crassa* and other fungal and nonfungal organisms provides a unique opportunity to examine the evolution of a specific intron on a larger scale.

It has been demonstrated that Δ*gna-1* strains form fewer protoperithecia than wild type and that these protoperithecia are "hairy," with an abundance of fringe hyphae on their surfaces. Importantly, no ascospore progeny are produced after application of opposite mating type conidia (39). The failure of Δ*gna-1* protoperithecia to develop into mature perithecia with ascospores could be explained by involvement of GNA-1 in a signaling pathway required for perithecial development. In this aspect, Δ*gna-1* strains display a defect similar to Δ*pre-1* mutants during development of perithecia (44). PRE-1 is one of two pheromone receptors required for chemotropism of female trichogynes toward male cells in *N. crassa*. In comparison to Δ*pre-1* mutants, the complexity of phenotypic defects during protoperithecial development and the block in perithecia formation observed in Δ*gna-1* strains indicate that multiple receptors must be coupled to GNA-1 during sexual development. The epistasis analysis between *gpr-1* and Gα genes rules out GNA-2 and GNA-3 acting downstream of GPR-1, leaving GNA-1 as a potential candidate for coupling to GPR-1. The genetic analysis using single and double mutants in the Δ*gna-1* background is complicated by the fact that GNA-1 is coupled to the pheromone receptors, and therefore deletion of *gna-1* causes a simultaneous block in the pheromone response path-

way (39, 44). Defects in protoperithecial development in Δ*gpr-1* Δ*gna-1* strains were identical to those observed in Δ*gna-1* mutants, consistent with GNA-1 acting downstream of GPR-1 for this trait. It is also possible that GPR-1 exerts its action in *N. crassa* independently of heterotrimeric G proteins, particularly during perithecial development. Accumulating evidence points to G-protein-independent activities for GPCRs in several systems (13, 15). Along these lines, it is noteworthy that a heterotrimeric G-protein-independent function has been proposed for *A. thaliana* GCR1 with respect to hormonal regulation of seed germination (19). Determination of possible G-protein-independent functions for *N. crassa* GPR-1 will require additional study.

Six putative homeodomain transcription factors have been annotated in *N. crassa* (12). Homeodomain proteins form a large superfamily of transcription factors fundamental to cellular proliferation, differentiation, and cell death in various species. Interestingly, deletion of the homeodomain transcription factor gene *bek-1* led to several defects in common with Δ*gpr-1* mutants, including the formation of ruptured perithecia lacking ostioles. Three TALE superclass homeobox genes have been identified in the genome of *S. cerevisiae* and have been grouped into the M-ATYPE and the CUP classes (16). One of the yeast homeobox proteins, Tos8p, targets promoter regions of genes that are involved in bud growth during G_1/S events (36). A TALE member, Pth12p, has been previously identified in the filamentous fungus *M. grisea* and has been shown to be involved in appressorium maturation (P. Hauck et al. [http://www.ncbi.nlm.nih.gov/entrez/viewer.fcgi?db = protein&val = 67005921]).

Some members of the TALE homeodomain protein family have been implicated as downstream targets of signal transduction pathways. It has been reported that protein kinase A strongly activates expression through PBX-HOX binding sites in HEK293 cells (human embryonic kidney epithelial cell line) (64), and protein kinase A transactivation domains were mapped to the MEIS1A and MEIS1B C termini (38). The MEIS protein forms stable heterodimers with the PBX homeodomain protein and binds to DNA in cooperation with a HOX partner (51). In a recent study, the ERK1/2 mitogen-activated protein kinase was shown to phosphorylate and negatively regulate the Arix/Phox2a homedomain protein (37). The epistasis analysis between *gpr-1* and *bek-1* indicates that BEK-1 possibly acts downstream of GPR-1 in *N. crassa*. However, the relationship between these two proteins remains unclear. We propose that the effect must be posttranscriptional, as the *bek-1* transcript level was not greatly affected in Δ*gpr-1* strains or vice versa. Further experimental work will be required to establish the molecular mechanism by which BEK-1 is regulated by the GPR-1 signaling pathway, including identification of potential partners, upstream regulators, and genes targeted by BEK-1.

Sexual development in *N. crassa* is a complex process for which molecular mechanisms are not well understood. Unfertilized and fertilized female reproductive structures consist of numerous different cell types (9). The mature perithecium is filled with asci (unbranched nonseptate hyphae) that contain ascospores and paraphyses (branched, multinucleate nonascogenous hyphae). The internal contents of the perithecium are enveloped by the outer perithecial wall, consisting of thick-walled pseudoparenchymatous cells (63). The cell types of the perithecial neck differ from the cells of the perithecial body. The ostiolar canal is lined with short branched cells (periphyses) which differentiate into pseudoparenchymatous neck wall cells (63). Upon maturation, a single ascus extends to the ostiole to discharge the ascospores (35). The actual mechanism of ascospore ejection has not been determined either in *N. crassa* or other ascomycetes. A recent study in *Giberella zeae* showed that three major osmolytes, mannitol, K^+, and Cl^-, were present in the epiplasmic fluid that is discharged along with ascospores but that potassium and chloride ions are likely the main osmolytes driving ascospore ejection (67).

Δ*gpr-1* strains display unique morphological defects (deformed beaks with no ostioles) that have not been previously reported in *N. crassa.* However, the isolation of two mutants that lack ostioles, *m* and *n*, has been reported for the ascomycete filamentous fungus *Sordaria macrospora* (26). The loss of ostioles dramatically compromises the ability of these fungi to disseminate progeny. In addition, Δ*gpr-1* mutants form beaks that are defective in phototropism (unpublished data). We speculate that the absence of ostioles stems from defects in development of periphyses and wall cells of the perithecial neck (63). Moreover, we cannot exclude the possibility that the volcano-shaped beaks and ruptured perithecia observed in Δ*gpr-1* mutants could result from an excess of turgor pressure inside perithecia of this strain. Therefore, future studies will require a multipronged approach to identify the molecular mechanism(s) underlying GPR-1 action. This includes identification and characterization of the cell types affected by loss of *gpr-1* during protoperithecial and perithecial development by using microscopic approaches, determination of the genes regulated by GPR-1 and BEK-1 during sexual development, and analysis of possible changes in concentration of osmolytic compounds in developing perithecia.

ACKNOWLEDGMENTS

We thank Nick Read and members of the Borkovich laboratory for many helpful discussions. We thank Michael Freitag and Eric Selker for plasmids pMF272 and pMF280. We acknowledge Carol Jones, Liande Li, Sara Martinez, and Gyungsoon Park for comments on the manuscript.

This work was supported by grant GM48626 from the National Institutes of Health to K.A.B.

REFERENCES

1. **Altschul, S. F., T. L. Madden, A. A. Schaffer, J. Zhang, Z. Zhang, W. Miller, and D. J. Lipman.** 1997. Gapped BLAST and PSI-BLAST: a new generation of protein database search programs. Nucleic Acids Res. **25:**3389–3402.
2. **Apone, F., N. Alyeshmerni, K. Wiens, D. Chalmers, M. J. Chrispeels, and G. Colucci.** 2003. The G-protein-coupled receptor GCR1 regulates DNA synthesis through activation of phosphatidylinositol-specific phospholipase C. Plant Physiol. **133:**571–579.
3. **Aramayo, R.** 1996. Gene replacement at the *his-3* locus of *Neurospora crassa*. Fungal Genet. Newsl. **43:**9–13.
4. **Baasiri, R. A., X. Lu, P. S. Rowley, G. E. Turner, and K. A. Borkovich.** 1997. Overlapping functions for two G protein alpha subunits in *Neurospora crassa*. Genetics **147:**137–145.
5. **Bell-Pedersen, D., J. C. Dunlap, and J. J. Loros.** 1996. Distinct *cis*-acting elements mediate clock, light, and developmental regulation of the *Neurospora crassa eas* (*ccg-2*) gene. Mol. Cell. Biol. **16:**513–521.
6. **Bieszke, J. A., E. L. Braun, L. E. Bean, S. Kang, D. O. Natvig, and K. A. Borkovich.** 1999. The *nop-1* gene of *Neurospora crassa* encodes a seven transmembrane helix retinal-binding protein homologous to archaeal rhodopsins. Proc. Natl. Acad. Sci. USA **96:**8034–8039.
7. **Bistis, G. N.** 1981. Chemotropic interactions between trichogynes and conidia of opposite mating-type in *Neurospora crassa*. Mycologia **73:**959–975.
8. **Bistis, G. N.** 1983. Evidence for diffusible, mating-type-specific trichogyne attractants in *Neurospora crassa*. Exp. Mycol. **7:**292–295.

9. **Bistis, G. N., D. D. Perkins, and N. D. Read.** 2003. Different cell types in *Neurospora crassa*. Fungal Genet. Newsl. **50:**17–19.
10. **Blumer, K. J., J. E. Reneke, and J. Thorner.** 1988. The *STE2* gene product is the ligand-binding component of the alpha-factor receptor of *Saccharomyces cerevisiae*. J. Biol. Chem. **263:**10836–10842.
11. **Bolker, M., M. Urban, and R. Kahmann.** 1992. The a mating type locus of *U. maydis* specifies cell signaling components. Cell **68:**441–450.
12. **Borkovich, K. A., L. A. Alex, O. Yarden, M. Freitag, G. E. Turner, N. D. Read, S. Seiler, D. Bell-Pedersen, J. Paietta, N. Plesofsky, M. Plamann, M. Goodrich-Tanrikulu, U. Schulte, G. Mannhaupt, F. E. Nargang, A. Radford, C. Selitrennikoff, J. E. Galagan, J. C. Dunlap, J. J. Loros, D. Catcheside, H. Inoue, R. Aramayo, M. Polymenis, E. U. Selker, M. S. Sachs, G. A. Marzluf, I. Paulsen, R. Davis, D. J. Ebbole, A. Zelter, E. R. Kalkman, R. O'Rourke, F. Bowring, J. Yeadon, C. Ishii, K. Suzuki, W. Sakai, and R. Pratt.** 2004. Lessons from the genome sequence of *Neurospora crassa*: tracing the path from genomic blueprint to multicellular organism. Microbiol. Mol. Biol. Rev. **68:**1–108.
13. **Brady, A. E., and L. E. Limbird.** 2002. G protein-coupled receptor interacting proteins: emerging roles in localization and signal transduction. Cell Signal. **14:**297–309.
14. **Bryson-Richardson, R. J., D. W. Logan, P. D. Currie, and I. J. Jackson.** 2004. Large-scale analysis of gene structure in rhodopsin-like GPCRs: evidence for widespread loss of an ancient intron. Gene **338:**15–23.
15. **Brzostowski, J. A., and A. R. Kimmel.** 2001. Signaling at zero G: G-protein-independent functions for 7-TM receptors. Trends Biochem. Sci. **26:**291–297.
16. **Burglin, T. R.** 1997. Analysis of TALE superclass homeobox genes (MEIS, PBC, KNOX, Iroquois, TGIF) reveals a novel domain conserved between plants and animals. Nucleic Acids Res. **25:**4173–4180.
17. **Case, M., M. Schweizer, S. Kushner, and N. Giles.** 1979. Efficient transformation of *Neurospora crassa* by utilizing hybrid plasmid DNA. Proc. Natl. Acad. Sci. USA **76:**5259–5263.
18. **Chang, Y. C., G. F. Miller, and K. J. Kwon-Chung.** 2003. Importance of a developmentally regulated pheromone receptor of *Cryptococcus neoformans* for virulence. Infect. Immun. **71:**4953–4960.
19. **Chen, J. G., S. Pandey, J. Huang, J. M. Alonso, J. R. Ecker, S. M. Assmann, and A. M. Jones.** 2004. GCR1 can act independently of heterotrimeric G-protein in response to brassinosteroids and gibberellins in *Arabidopsis* seed germination. Plant Physiol. **135:**907–915.
20. **Chenna, R., H. Sugawara, T. Koike, R. Lopez, T. J. Gibson, D. G. Higgins, and J. D. Thompson.** 2003. Multiple sequence alignment with the Clustal series of programs. Nucleic Acids Res. **31:**3497–3500.
21. **Chung, S., M. Karos, Y. C. Chang, J. Lukszo, B. L. Wickes, and K. J. Kwon-Chung.** 2002. Molecular analysis of *CPR*α, a *MAT*α-specific pheromone receptor gene of *Cryptococcus neoformans*. Eukaryot. Cell **1:**432–439.
22. **Colot, H., G. Park, G. Turner, C. Ringelberg, C. Crew, L. Litvinkova, R. Weiss, K. Borkovich, and J. Dunlap.** 2006. A high-throughput gene knockout procedure for *Neurospora* reveals functions for multiple transcription factors. Proc. Natl. Acad. Sci. USA **103:**10352–10357.
23. **Colucci, G., F. Apone, N. Alyeshmerni, D. Chalmers, and M. J. Chrispeels.** 2002. *GCR1*, the putative *Arabidopsis* G-protein-coupled receptor gene is cell cycle-regulated, and its overexpression abolishes seed dormancy and shortens time to flowering. Proc. Natl. Acad. Sci. USA **99:**4736–4741.
24. **Davis, R. H., and F. J. deSerres.** 1970. Genetic and microbiological research techniques for *Neurospora crassa*. Methods Enzymol. **71A:**79–143.
25. **Ebbole, D. J., and M. S. Sachs.** 1990. A rapid and simple method for isolation of *Neurospora crassa* homokaryons using microconidia. Fungal Genet. Newsl. **37:**17–18.
26. **Esser, K., and J. Straub.** 1958. Genetic studies on *Sordaria macrospora* Auersw., compensation and induction in gene-dependent developmental defects. Z. Vererbungsl. **89:**729–746. (In German.)
27. **Folco, H. D., M. Freitag, A. Ramon, E. D. Temporini, M. E. Alvarez, I. Garcia, C. Scazzocchio, E. U. Selker, and A. L. Rosa.** 2003. Histone H1 Is required for proper regulation of pyruvate decarboxylase gene expression in *Neurospora crassa*. Eukaryot. Cell **2:**341–350.
28. **Galagan, J. E., S. E. Calvo, K. A. Borkovich, E. U. Selker, N. D. Read, D. Jaffe, W. FitzHugh, L. J. Ma, S. Smirnov, S. Purcell, B. Rehman, T. Elkins, R. Engels, S. Wang, C. B. Nielsen, J. Butler, M. Endrizzi, D. Qui, P. Ianakiev, D. Bell-Pedersen, M. A. Nelson, M. Werner-Washburne, C. P. Selitrennikoff, J. A. Kinsey, E. L. Braun, A. Zelter, U. Schulte, G. O. Kothe, G. Jedd, W. Mewes, C. Staben, E. Marcotte, D. Greenberg, A. Roy, K. Foley, J. Naylor, N. Stange-Thomann, R. Barrett, S. Gnerre, M. Kamal, M. Kamvysselis, E. Mauceli, C. Bielke, S. Rudd, D. Frishman, S. Krystofova, C. Rasmussen, R. L. Metzenberg, D. D. Perkins, S. Kroken, C. Cogoni, G. Macino, D. Catcheside, W. Li, R. J. Pratt, S. A. Osmani, C. P. DeSouza, L. Glass, M. J. Orbach, J. A. Berglund, R. Voelker, O. Yarden, M. Plamann, S. Seiler, J. Dunlap, A. Radford, R. Aramayo, D. O. Natvig, L. A. Alex, G. Mannhaupt, D. J. Ebbole, M. Freitag, I. Paulsen, M. S. Sachs, E. S. Lander, C. Nusbaum, and B. Birren.** 2003. The genome sequence of the filamentous fungus *Neurospora crassa*. Nature **422:**859–868.
29. **Geerts, D., N. Schilderink, G. Jorritsma, and R. Versteed.** 2003. The role of the *MEIS* homeobox genes in neuroblastoma. Cancer Lett. **197:**87–92.
30. **Gehring, W. J., M. Affolter, and T. Burglin.** 1994. Homeodomain proteins. Annu. Rev. Biochem. **63:**487–526.
31. **Hagen, D. C., G. McCaffrey, and G. F. Sprague, Jr.** 1986. Evidence the yeast *STE3* gene encodes a receptor for the peptide pheromone a-factor: gene sequence and implications for the structure of the presumed receptor. Proc. Natl. Acad. Sci. USA **83:**1418–1422.
32. **Han, K. H., J. A. Seo, and J. H. Yu.** 2004. A putative G-protein-coupled receptor negatively controls sexual development in *Aspergillus nidulans*. Mol. Microbiol. **51:**1333–1345.
33. **Hanahan, D.** 1983. Studies on transformation of *Escherichia coli* with plasmids. J. Mol. Biol. **166:**557–580.
34. **Harding, R. W., and S. Melles.** 1983. Genetic analysis of phototropism of *Neurospora crassa* perithecial beaks using white collar and albino mutants. Plant Physiol. **72:**996–1000.
35. **Harris, J. L., H. B. Howe, Jr., and I. L. Roth.** 1975. Scanning electron microscopy of surface and internal features of developing perithecia of *Neurospora crassa*. J. Bacteriol. **122:**1239–1246.
36. **Horak, C. E., N. M. Luscombe, J. Qian, P. Bertone, S. Piccirrillo, M. Gerstein, and M. Snyder.** 2002. Complex transcriptional circuitry at the G1/S transition in *Saccharomyces cerevisiae*. Genes Dev. **16:**3017–3033.
37. **Hsieh, M. M., G. Lupas, J. Rychlik, S. Dziennis, B. A. Habecker, and E. J. Lewis.** 2005. ERK1/2 is a negative regulator of homeodomain protein Arix/Phox2a. J. Neurochem. **94:**1719–1727.
38. **Huang, H., M. Rastegar, C. Bodner, S. L. Goh, I. Rambaldi, and M. Featherstone.** 2005. MEIS C termini harbor transcriptional activation domains that respond to cell signaling. J. Biol. Chem. **280:**10119–10127.
39. **Ivey, F. D., P. N. Hodge, G. E. Turner, and K. A. Borkovich.** 1996. The G alpha i homologue *gna-1* controls multiple differentiation pathways in *Neurospora crassa*. Mol. Biol. Cell **7:**1283–1297.
40. **Ivey, F. D., Q. Yang, and K. A. Borkovich.** 1999. Positive regulation of adenylyl cyclase activity by a $G\alpha_i$ homolog in *Neurospora crassa*. Fungal Genet. Biol. **26:**48–61.
41. **Josefsson, L. G., and L. Rask.** 1997. Cloning of a putative G-protein-coupled receptor from *Arabidopsis thaliana*. Eur. J. Biochem. **249:**415–420.
42. **Kays, A. M., and K. A. Borkovich.** 2004. Severe impairment of growth and differentiation in a *Neurospora crassa* mutant lacking all heterotrimeric G alpha proteins. Genetics **166:**1229–1240.
43. **Kays, A. M., P. S. Rowley, R. A. Baasiri, and K. A. Borkovich.** 2000. Regulation of conidiation and adenylyl cyclase levels by the Gα protein GNA-3 in *Neurospora crassa*. Mol. Cell. Biol. **20:**7693–7705.
44. **Kim, H., and K. A. Borkovich.** 2004. A pheromone receptor gene, *pre-1*, is essential for mating type-specific directional growth and fusion of trichogynes and female fertility in *Neurospora crassa*. Mol. Microbiol. **52:**1781–1798.
45. **Kim, H., and K. A. Borkovich.** 2006. Pheromones are essential for male fertility and sufficient to direct chemotropic polarized growth of trichogynes during mating in *Neurospora crassa*. Eukaryot. Cell **5:**544–554.
46. **Klein, P. S., T. J. Sun, C. L. Saxe III, A. R. Kimmel, R. L. Johnson, and P. N. Devreotes.** 1988. A chemoattractant receptor controls development in *Dictyostelium discoideum*. Science **241:**1467–1472.
47. **Krystofova, S., and K. A. Borkovich.** 2005. The heterotrimeric G-protein subunits GNG-1 and GNB-1 form a Gβγ dimer required for normal female fertility, asexual development, and Gα protein levels in *Neurospora crassa*. Eukaryot. Cell **4:**365–378.
48. **Lengeler, K. B., R. C. Davidson, C. D'Souza, T. Harashima, W. C. Shen, P. Wang, X. Pan, M. Waugh, and J. Heitman.** 2000. Signal transduction cascades regulating fungal development and virulence. Microbiol. Mol. Biol. Rev. **64:**746–785.

48a. **Li, L., and K. A. Borkovich.** 2006. GPR-4 is a predicted G-protein-coupled receptor required for carbon source-dependent asexual growth and development in *Neurospora crassa*. **5:**1287–1300.

49. **Maidan, M. M., L. De Rop, J. Serneels, S. Exler, S. Rupp, H. Tournu, J. M. Thevelein, and P. Van Dijck.** 2005. The G-protein-coupled receptor Gpr1 and the Gα protein Gpa2 act through the cAMP-protein kinase A pathway to induce morphogenesis in *Candida albicans*. Mol. Biol. Cell **16:**1971–1986.
50. **Maidan, M. M., J. M. Thevelein, and P. Van Dijck.** 2005. Carbon source induced yeast-to-hypha transition in *Candida albicans* is dependent on the presence of amino acids and on the G-protein-coupled receptor Gpr1. Biochem. Soc. Trans. **33:**291–293.
51. **Mann, R. S., and M. Affolter.** 1998. Hox proteins meet more partners. Curr. Opin. Genet. Dev. **8:**423–429.
52. **Miwa, T., Y. Takagi, M. Shinozaki, C. W. Yun, W. A. Schell, J. R. Perfect, H. Kumagai, and H. Tamaki.** 2004. Gpr1, a putative G-protein-coupled receptor, regulates morphogenesis and hypha formation in the pathogenic fungus *Candida albicans*. Eukaryot. Cell **3:**919–931.
53. **Neves, S. R., P. T. Ram, and R. Iyengar.** 2002. G protein pathways. Science **296:**1636–1639.
54. **Olesnicky, N. S., A. J. Brown, S. J. Dowell, and L. A. Casselton.** 1999. A constitutively active G-protein-coupled receptor causes mating self-compatibility in the mushroom *Coprinus*. EMBO J. **18:**2756–2763.
55. **Orbach, M. J.** 1994. A cosmid with a HyR marker for fungal library construction and screening. Gene **150:**159–162.
56. **O'Shea, S. F., P. T. Chaure, J. R. Halsall, N. S. Olesnicky, A. Leibbrandt,**

I. F. Connerton, and L. A. Casselton. 1998. A large pheromone and receptor gene complex determines multiple B mating type specificities in *Coprinus cinereus*. Genetics **148:**1081–1090.
57. **Pall, M. L.** 1993. The use of ignite (basta; glufosinate; phosphinothricin) to select transformants of bar-containing plasmids in *Neurospora crassa*. Fungal Genet. Newsl. **40:**58.
58. **Pall, M. L., and J. P. Brunelli.** 1993. A series of six compact fungal transformation vectors containing polylinkers with multiple unique restriction sites. Fungal Genet. Newsl **40:**59–62.
59. **Pandey, S., and S. M. Assmann.** 2004. The *Arabidopsis* putative G-protein-coupled receptor GCR1 interacts with the G protein alpha subunit GPA1 and regulates abscisic acid signaling. Plant Cell **16:**1616–1632.
60. **Plakidou-Dymock, S., D. Dymock, and R. Hooley.** 1998. A higher plant seven-transmembrane receptor that influences sensitivity to cytokinins. Curr. Biol. **8:**315–324.
61. **Raisley, B., M. Zhang, D. Hereld, and J. A. Hadwiger.** 2004. A cAMP receptor-like G protein-coupled receptor with roles in growth regulation and development. Dev. Biol. **265:**433–445.
62. **Raju, N. B.** 1992. Genetic control of the sexual cycle in *Neurospora*. Mycol. Res. **96:**241–262.
63. **Read, N., and A. Beckett.** 1985. The anatomy of the mature perithecium in *Sordaria humana* and its significance for fungal multicellular development. Can. J. Bot. **63:**281–296.
64. **Saleh, M., I. Rambaldi, X. J. Yang, and M. S. Featherstone.** 2000. Cell signaling switches HOX-PBX complexes from repressors to activators of transcription mediated by histone deacetylases and histone acetyltransferases. Mol. Cell. Biol. **20:**8623–8633.
65. **Seo, J. A., K. H. Han, and J. H. Yu.** 2004. The *gprA* and *gprB* genes encode putative G protein-coupled receptors required for self-fertilization in *Aspergillus nidulans*. Mol. Microbiol. **53:**1611–1623.
66. **Tanaka, K., J. Davey, Y. Imai, and M. Yamamoto.** 1993. *Schizosaccharomyces pombe map3*+ encodes the putative M-factor receptor. Mol. Cell. Biol. **13:**80–88.
67. **Trail, F., I. Gaffoor, and S. Vogel.** 2005. Ejection mechanics and trajectory of the ascospores of *Gibberella zeae* (anamorph *Fusarium graminearum*). Fungal Genet. Biol. **42:**528–533.
68. **Turner, G. E., and K. A. Borkovich.** 1993. Identification of a G protein alpha subunit from *Neurospora crassa* that is a member of the Gi family. J. Biol. Chem. **268:**14805–14811.
69. **Vann, D.** 1995. Electroporation-based transformation of freshly harvested conidia of *Neurospora crassa*. Fungal Genet. Newsl. **42A:**53.
70. **Vogel, H.** 1964. Distribution of lysine pathways among fungi: evolutionary implications. Am. Nat. **98:**435–446.
71. **Welton, R. M., and C. S. Hoffman.** 2000. Glucose monitoring in fission yeast via the gpa2 Gα, the git5 Gβ and the git3 putative glucose receptor. Genetics **156:**513–521.
72. **Wendland, J., L. J. Vaillancourt, J. Hegner, K. B. Lengeler, K. J. Laddison, C. A. Specht, C. A. Raper, and E. Kothe.** 1995. The mating-type locus *B alpha* 1 of *Schizophyllum commune* contains a pheromone receptor gene and putative pheromone genes. EMBO J. **14:**5271–5278.
73. **Westergaard, M., and H. Mitchell.** 1947. *Neurospora* V. A synthetic medium favoring sexual reproduction. Am. J. Bot. **34:**573–577.
74. **Xue, C., Y. S. Bahn, G. M. Cox, and J. Heitman.** 2006. G protein-coupled receptor Gpr4 senses amino acids and activates the cAMP-PKA pathway in *Cryptococcus neoformans*. Mol. Biol. Cell **17:**667–679.
75. **Xue, Y., M. Battle, and J. P. Hirsch.** 1998. *GPR1* encodes a putative G protein-coupled receptor that associates with the Gpa2p Galpha subunit and functions in a Ras-independent pathway. EMBO J. **17:**1996–2007.
76. **Yang, Q., and K. A. Borkovich.** 1999. Mutational activation of a $G\alpha_i$ causes uncontrolled proliferation of aerial hyphae and increased sensitivity to heat and oxidative stress in *Neurospora crassa*. Genetics **151:**107–117.
77. **Yang, Q., S. I. Poole, and K. A. Borkovich.** 2002. A G-protein β subunit required for sexual and vegetative development and maintenance of normal Gα protein levels in *Neurospora crassa*. Eukaryot. Cell **1:**378–390.
78. **Yun, C. W., H. Tamaki, R. Nakayama, K. Yamamoto, and H. Kumagai.** 1997. G-protein coupled receptor from yeast *Saccharomyces cerevisiae*. Biochem. Biophys. Res. Commun. **240:**287–292.
79. **Yun, C. W., H. Tamaki, R. Nakayama, K. Yamamoto, and H. Kumagai.** 1998. Gpr1p, a putative G-protein-coupled receptor, regulates glucose-dependent cellular cAMP level in yeast *Saccharomyces cerevisiae*. Biochem. Biophys. Res. Commun. **252:**29–33.